



**Universiteit  
Leiden**  
The Netherlands

## **Iron-immune interactions in Alzheimer's disease**

Kenkhuis, B.

### **Citation**

Kenkhuis, B. (2022, June 8). *Iron-immune interactions in Alzheimer's disease*. Retrieved from <https://hdl.handle.net/1887/3307816>

Version: Publisher's Version

License: [Licence agreement concerning inclusion of doctoral thesis in the Institutional Repository of the University of Leiden](#)

Downloaded from: <https://hdl.handle.net/1887/3307816>

**Note:** To cite this publication please use the final published version (if applicable).

# Part I

# Translational MRI



# Chapter 2

## Post-mortem MRI and histopathology in neurologic disease: a translational approach

---

Laura E. Jonkman, Boyd Kenkhuis, Jeroen J.G. Geurts, Wilma D.J. van de Berg,

Neuroscience Bulletin **35**, 229-243 (2019)

**Abstract**

In this review, combined post-mortem brain MRI and histology studies are highlighted, illustrating the relevance of translational approaches to define novel MRI signatures of neuropathological lesions in neuroinflammatory and neurodegenerative disorders. Initial studies combining post-mortem MRI and histology validated various MRI sequences, assessing their sensitivity and specificity as diagnostic biomarker in neurologic disease. More recent studies focussed on defining new radiological (bio) markers and implementing them in the clinical (research) setting. By combining neurologic and neuroanatomical expertise with radiological development and pathological validation, a cycle emerges that allows for discovery of (novel) MRI biomarkers to be implemented in vivo. Examples of this cycle are presented for multiple sclerosis, Alzheimer's disease, Parkinson's disease and traumatic brain injury. Some applications have shown to be successful, while others require further validation. In conclusion, there is much to explore with post-mortem MRI and histology studies, which can eventually be of high relevance for clinical practice.

## Introduction

MRI is routinely used in clinical practice to evaluate brain anatomy and pathology in neuroinflammatory and neurodegenerative disorders, to aid (differential) diagnosis or assess disease severity, e.g. estimating atrophy in Alzheimer's disease (AD) or lesion load in multiple sclerosis (MS). Knowledge of the histopathological substrate of these radiological findings can come with a delay; an in-vivo MRI is made, and only after death (months or years later) radiological findings can be validated at pathological inspection<sup>1-4</sup>. With the emergence of post-mortem MRI with subsequent histopathological validation of the same donor brain, this delay is no longer a hurdle and various MRI sequences can be assessed for their pathological sensitivity and specificity (see Fig. 1 in blue)<sup>5-7</sup>.

Importantly, combined post-mortem MRI and histopathology can be used beyond mere validation. It can aid development of new MRI sequences to detect more subtle pathology in-vivo (see Fig. 1 in orange), and address more complicated differential diagnosis conundrums, e.g. differentiating Parkinson's disease (PD) from other parkinsonisms<sup>8</sup>. As such, an interplay emerges between clinical practice, radiological development and pathological validation, to eventually establish a sensitive and specific radiological diagnostic or prognostic (bio)marker that can be implemented in the clinical (research) setting (see Fig. 1, full circle).

This review will focus on studies using post-mortem MRI and histopathology, working towards clinical applicability of novel MRI (bio)markers of neuropathological lesions. First, we will discuss the essentials and logistics of setting up an efficient post-mortem MRI and histology pipeline. Then we will highlight examples of combined post-mortem MRI and histopathology studies in four neurological diseases - multiple sclerosis (MS), Alzheimer's disease (AD), Parkinson's disease (PD) and traumatic brain injury (TBI) – where are they within the cycle of validation and (clinical research) implementation?

## Post-mortem MRI and histopathology pipeline

Donors for post-mortem brain research are generally recruited through brain banks or body bequest programs after informed consent of the donor for brain autopsy and use of material for research purposes. All procedures of the brain bank have to be approved by a local medical ethical committee. To maintain a high quality of tissue integrity, a short post-mortem delay (PMD; time between death and formalin fixation) is crucial. When in situ post-mortem MRI (brain still in cranium) or ex vivo MRI with fresh tissue is added into the equation, this may pose an extra challenge. Therefore, an adequate logistic setup is required to prevent unnecessary delays.

Logistics regarding brain autopsy programs without MRI have previously been

described<sup>9–12</sup>. We will briefly describe the procedures when both in situ and ex vivo MRI are included in the protocol, as done by the Normal Aging brain Collection Amsterdam (NABCA; <http://nabca.eu>), an initiative of the department of Anatomy and Neurosciences of the VU university medical center, which includes non-neurological donors, and neurological donors in close collaboration with the Netherlands Brain Bank (NBB; <http://brainbank.nl>). This pipeline is based on the Amsterdam protocol as previously described for MS research<sup>13</sup>.

After death, the donor is transported to the mortuary of the hospital. There, a team consisting of an MRI researcher and autopsy assistant transport the donor to the MRI scanner and include various conventional and advanced MRI sequences. Upon return to the mortuary, a neuropathologist and autopsy assistant perform the craniotomy and subsequent brain dissection according to a strict standardized protocol. At this time, only the left hemisphere is dissected and tissue blocks are snap frozen in liquid nitrogen allowing subsequent genetic, molecular and biochemical analysis. The right hemisphere is immersed in 4% buffered formalin for four weeks, after which it is scanned ex vivo at 7T MRI. After this ultra-high field MRI scan, the right hemisphere is dissected according to the Brain Net Europe protocol (BNE)<sup>9</sup> and tissue blocks are paraffin embedded. A selection of these brain tissue blocks is used for a comprehensive neuropathological assessment of lesions defining various neurological diseases, such as (subtypes of) dementia, PD and MS. Patient data, including demographics, medical history, radiological and neuropathological information, are combined in a donor report.

Additions to this protocol may occur, for instance by means of an ex vivo scan of brain slices after craniotomy, upon which MRI guided tissue dissection can take place (as done in MS donors for dissection of specific lesions<sup>13</sup>). Another option is to obtain formalin fixed brain slices or tissue blocks at autopsy, which are used for ultra-high MRI at a later stage. After embedding of tissue, the brain tissue can be stained for a range of (immuno)histochemical markers to assess correlation between MRI signal intensities and morphometric or pathological changes.

In research studies, regions of interest are generally marked on MRI, and histological sections are matched to the corresponding MRI plane, using as many anatomical landmarks (border of the white and gray matter, sulci, gyri and ventricles) as available. Alternatively, MRI atlases can be used or designed, depending on the research question.

### **Post-mortem MRI and histology in multiple sclerosis**

MS is characterized by multifocal lesions in the white matter (WM), grey matter (GM), hippocampus, cerebellum, deep grey nuclei, and spinal cord. These lesions have various degrees of inflammation, demyelination and other histopathological



characteristics<sup>14,15</sup>. MRI has considerably contributed to the understanding and early diagnosis of MS and is routinely used to monitor disease course and progression<sup>16,17</sup>. Since the early 2000s, post-mortem MRI in MS has also contributed to the interpretation of MRI abnormalities with respect to their underlying histopathology, in both white and gray matter. We will address these findings in the next paragraphs.

#### *White matter lesions and remyelination in MS*

White matter lesions in MS are generally well visible on conventional MRI (e.g. (gadolinium-)T1, T2 and proton-density (PD)). However, lesion stage, specifically remyelination, cannot be assessed on these conventional MRI images. Remyelination can be defined as thin myelin sheets occurring at the edge or throughout a lesion.<sup>18</sup> For monitoring of treatment effects it would be beneficial to monitor remyelination and distinguish it from demyelination and surrounding normal appearing white matter (NAWM). Therefore, several studies have looked at distinguishing de- and remyelination with quantitative post-mortem MRI and subsequent histological validation of matched tissue type<sup>18,19</sup>. These studies showed that some distinction could be made, especially between remyelination and demyelination, but not between remyelination and NAWM<sup>19</sup>. Although remyelinated tissue had signal intensities in between demyelination and NAWM, the three groups (NAWM, demyelination and remyelination) had overlapping quantitative MRI values<sup>18</sup>. Within the cycle of Fig. 1, radiological optimization was not fully successful, indicating a limited clinical value for distinguishing and monitoring remyelination. Investigating this method at higher field strength may yield better results that may subsequently be implemented in the MS in vivo setting.

A study by Yao et al.<sup>20</sup> included quantitative MRI at ultra-high field strength, namely 7T and 11.7T, with histology to characterize the pathological features of iron and myelin in WM lesions. They found that while R2\*reduction (inverse transverse relaxation time constant) corresponded to severe loss of both iron and myelin, a negative phase shift (of susceptibility-weighted images) corresponded to focal iron accumulation<sup>20</sup>. This indicates a differential pathological sensitivity of R2\* and negative phase shift (for myelin and iron respectively). The results of this pathological validation has yet to show its clinical applicability.

#### *Gray matter lesions in MS*

Cortical gray matter lesions, in contrast to lesions of the white matter, are generally characterized by an intact blood-brain barrier and a lack of inflammatory cell infiltration<sup>21,22</sup> and relate to physical disability, cognition and disease progression<sup>23–25</sup>. One of the first post-mortem MRI and histology studies, at 0.6T, showed that cortical lesions, as scored on MRI, were dramatically under-reported when directly compared to histology of the same brain slice<sup>26</sup>. In subsequent years, with conventional MRI sequences at 1.5T, only up to 5% of histopathological defined cortical lesions could be detected<sup>27</sup>. To increase lesion detection rates, new MRI sequences were developed.

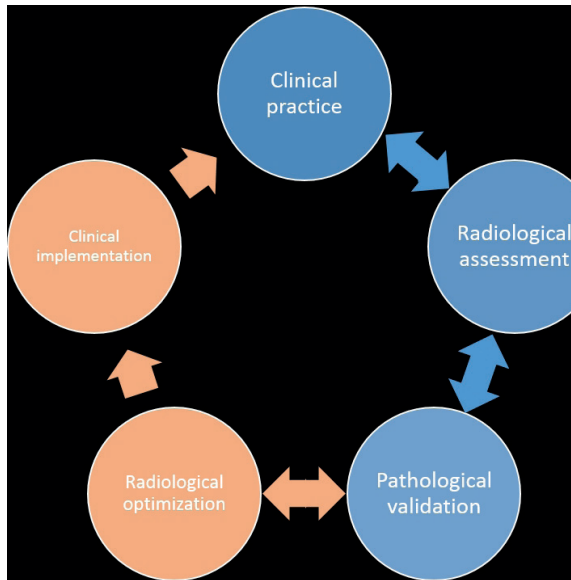


**Fig. 1 Cycle for integration of radiological and pathological development into clinical (research) practice.** Clinical practice uses radiological assessment (MRI) to assess structural brain changes in patients with neuroinflammatory and neurodegenerative disorders. Initial post-mortem MRI and histopathological studies focussed on validating MRI sequences for their pathological sensitivity and specificity (blue sections). However, more recent studies focus on optimizing and developing MRI sequences to define more sensitive MRI measures to improve diagnostic and prognostic diagnosis in clinical setting (orange sections). As such, post-mortem MRI is of high interest to translate MRI features in histopathological terms but also in translating knowledge on the type or distribution of pathological lesions to MRI, thereby integrating clinical practice, radiological development and pathological validation to establish optimal radiological (bio)markers (whole circle).

Such as a phase-sensitive inversion recovery (PSIR) or double inversion recovery (DIR) sequence, the latter suppresses the signal of both the CSF and WM, thereby allowing better visualization of the cortex. Nevertheless, even with these newly developed sequences, approximately 82% of cortical lesions remained undetected by MRI as seen by Seewann and colleagues in a post-mortem MRI with subsequent histology study<sup>28</sup>.

An increase in field strength was the next logical step as this could increase the signal-to-noise ratio and spatial resolution. Initial studies comparing DIR at 1.5T and 3T showed improved cortical lesion detection by 192% with 3T DIR<sup>29</sup>. The pathological specificity of DIR was also tested in a study comparing a DIR and FLAIR sequence, in which DIR showed its superiority over FLAIR in detecting cortical lesions in MS (see Fig. 2)<sup>28</sup>. This led to the publication of consensus recommendations for MS cortical lesions scoring using DIR<sup>30</sup> which are used in multicenter settings using similar protocols. A good example of radiological development of MRI to better reflect histology, and implementation in the clinical setting (Fig. 1).

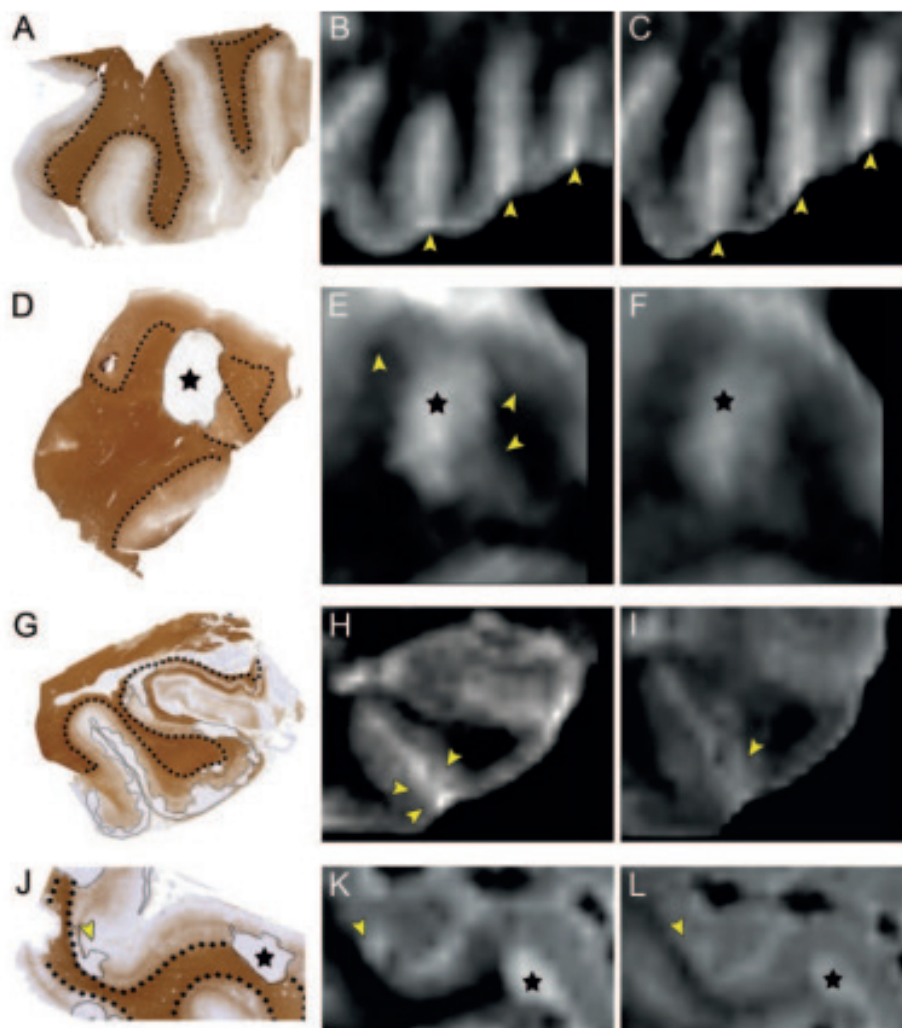


**Fig. 2** Examples of postmortem MRI at 1.5 T, with corresponding histopathology. (A, D, G, J) Proteolipid protein (PLP) stained tissue sections; dotted lines indicate borders between white and gray matter; cortical lesions are encircled by thin black lines. (B, E, H, K) Postmortem 3D double inversion recovery (DIR) images corresponding with the tissue sections. (C, F, I, L) Corresponding 3D fluid-attenuated inversion recovery (FLAIR) images. (A–C) Multiple sclerosis (MS) cortex with rather inhomogeneous signal intensity on MRI, but without any demyelinated lesions. The bright signal indicated by the arrowheads (B, C) is caused by blood and other fluid within the sulci, which should not be mistaken for subpial (type III) cortical pathology. (D–F) Mixed gray-white matter (type I) lesion (asterisk), which is seen on both 3D DIR and 3D FLAIR images. However, the gray matter border (arrowheads in E) is often easier identified on 3D DIR (E) as compared to 3D FLAIR (F). (G–I) Subpial (type III) cortical lesions (indicated by thin line in G and arrowheads in H and I) are slightly more conspicuous on 3D DIR (H) than on 3D FLAIR (I). (J–L) Mixed gray-white matter (type I) lesion (asterisks). Arrowhead in J–L: an intracortical lesion, which was prospectively scored on 3D DIR (K) and only retrospectively (i.e., with knowledge of histopathology) on 3D FLAIR (L). Reprint with permission from Wolters Kluwer Health.<sup>28</sup>

Although ~18% visibility with 3T DIR was an increase from the ~5% with conventional MRI, the question remained if this percentage could be further increased, perhaps by further increasing the field strength. One large post-mortem MRI study compared five sequences (DIR, FLAIR, T2, T2\*, T1) at two field strengths (3T and 7T). Results from this study showed that only 7T FLAIR and T2\* detected significantly more cortical lesions compared to 3T FLAIR and T2\* respectively<sup>31</sup>. Sensitivity of 7T MRI was ~28% when the MRI rater was blinded to histological data. However, when the MRI rater saw the histopathology of the same brain slice, and then looked back at MRI, sensitivity rates went up to ~84%<sup>32</sup>. This effect of increased retrospective sensitivity after knowing lesion type and location, was also found in another study<sup>33</sup>. It has been suggested that continuous observer training (with histological validation) on which signal changes may indicate a lesion, rather than a further increase in field strength, could possibly increase prospective cortical lesion detection<sup>32</sup>.

### **Post-mortem MRI and histology in Alzheimer's disease**

Alzheimer's Disease (AD), a neurodegenerative disorder characterized by memory disturbances, can only be diagnosed with absolute certainty via neuropathological examination of hallmarks Amyloid Beta-plaques (A $\beta$ ) and (p-)tau neurofibrillary tangles (NFT). In both clinical- and research settings, diagnosis is generally based on CSF biomarkers, MRI and clinical symptoms, but unfortunately accuracy is still unsatisfactory<sup>34</sup>. The AD research field has shown great interest in MRI as a possible biomarker for diagnosis, due to its potential to detect atrophy and pathological hallmarks non-invasively in an *in vivo* setting. Therefore, post-mortem MRI-pathology studies are extremely valuable, as they can verify the histological substrate of the observed contrast via direct comparison.

#### *Atrophy in AD*

Apostolova and colleagues explicitly endorse "the need for pathologic validation of clinical diagnostic criteria and any and all biomarker proposed to be useful for diagnosing AD or tracking its course over time."<sup>35</sup> Hippocampal atrophy is the most widely used MRI biomarker for AD to date, differentiating and predicting AD from non-neurological controls<sup>36,37</sup>, as well as AD from mild cognitive impairment (MCI)<sup>38,39</sup>. An initial study exploring the pathological validation of hippocampal atrophy found a negative relationship between ante-mortem hippocampal volume and post-mortem Braak and Braak staging<sup>40</sup>. A more recent study scanned hippocampi *ex vivo* at 7T and investigated hippocampal volume in relationship to burden of A $\beta$  and phosphorylated (p-)tau as well as neuronal count. In addition to a relationship with Braak and Braak staging, they found associations between hippocampal volume and (p-)tau, A $\beta$  burden and neuronal count. Additionally, some regional associations were found; A $\beta$  in Cornu Ammonis (CA)1 and subiculum lead to a decrease in global hippocampal volume, as well as (p-)tau in CA2 and CA3, and neuronal count in CA1,

CA3, and CA4<sup>35</sup>. Since within-subfield segmentation of the hippocampus is still challenging (even at 7T)<sup>41</sup>, correlations between hippocampal sub-region volume and pathological burden has yet to be undertaken and its clinical relevance to be determined.

#### *Parenchymal pathology in AD*

Ultra-high field MRI provides sufficient spatial resolution and signal-to-noise ratio needed to image A $\beta$  plaques, but not NFT's. Already in 1999, Benveniste and colleagues found that hypointensities seen on ex vivo T2\*-weighted MRI corresponded with neuritic plaques<sup>42</sup>. The close relationship between MRI contrast and A $\beta$  plaques was later confirmed in both human AD patients and APP/PS1 mice via direct comparison of 7T T2\* images and histology, using specifically designed histological coils<sup>43,44</sup>. However, further analysis of A $\beta$  plaques suggested that increased iron was responsible for the inherent contrast. Nabuurs and colleagues studied the MRI properties of the different cerebral A $\beta$  plaques, and found that fibrillary A $\beta$  (Congo Red positive), present in both vascular and parenchymal focal A $\beta$  plaques, but not in diffuse plaques, induce significant changes in T2\* and T2 signal. Diffuse A $\beta$  remained visually and quantitatively undetected with T2 and T2\* (see Fig. 3)<sup>45</sup>. This indicated that both iron and fibrillar A $\beta$  contribute to the observed hypointense signal on ex vivo MRI. Nevertheless, accurate in vivo detection of A $\beta$ -plaques is yet to be achieved.

Aside from the pathological hallmarks of A $\beta$  and NFT, Zeineh and colleagues investigated the contribution of microglia and iron to signal intensity changes at 7T. With the use of ex vivo MRI of 0.1mm isotropic resolution and co-registration with successive histological triple stains for iron, A $\beta$  and CD163 (a microglial marker), they were able to establish iron accumulation inside activated microglia to be responsible for the observed MR hypointensities, primarily inside the subiculum<sup>46</sup>. Since all cases were late stage AD, future work should elucidate the role of microglia and iron across the spectrum of non-neurological controls, mild cognitive impairment and AD.

Using ultra-high field MRI on small tissue samples of the frontal cortex, altered contrast of cortical texture was observed in AD patients. Pixel wise spatial correlation of signal intensity was calculated based on histology-MRI registration, and showed that the altered contrast could be explained by a combination of increased iron and changes in cortical myelin. Furthermore, this study showed that neuropathological correlates of early and late onset AD were distinguishable on 7T T2\* MRI<sup>47</sup>. Nevertheless, its utility for clinical applications needs to be further investigated.

More recent studies elaborated on this work by investigating changes in cortical texture in brain imaging, and by verifying its relationship with cortical myelo- and cytoarchitecture. In the study by Kenkhuis and colleagues, they characterized the visibility of myelo-architectural changes in AD patients and subsequently investigated the pathological substrate of cortical laminar alterations. Increased variability in

visible cortical lamination and severely disturbed cortical lamination was observed in the medial temporal lobe of AD patients. Upon histological inspection of these cases, correspondence with diffuse myelin-associated iron accumulation and A $\beta$ -associated iron deposits was found<sup>48</sup>.

### *Vascular pathology in AD*

Additional to parenchymal pathology, cerebrovascular disease (CVD) plays an important role in cognitive decline and dementia. At autopsy, the majority of AD patients exhibit cerebral amyloid angiopathy (CAA) and/or small vessel disease (SVD),<sup>49</sup> which include lacunar infarcts, white matter hyperintensities (WMH), microbleeds and cerebral microinfarcts (CMI).<sup>50</sup>

CAA is caused by A $\beta$  deposits within predominantly leptomeningeal and intracortical arteries, arterioles and capillaries<sup>51</sup>. Vascular A $\beta$  depositions have been suggested to cause microvascular lesions including microbleeds and CMI's, though definitive evidence remains absent<sup>52-55</sup>. As mentioned earlier, fibrillary A $\beta$  inside vascular A $\beta$  depositions can cause significant changes in T2\* and T2 signal<sup>45</sup>. However, when imaging CAA in AD, predominantly the harmful microvascular lesions are being imaged, which will be discussed in the following paragraphs.

WMH are predominantly of ischemic origin, but also non-ischemic demyelinated areas were reported<sup>56</sup>. They are easily detectable patches of increased hyperintense signal on T2\* MRI and are commonly seen in elderly patients. Literature suggests that WMHs predict AD prior to the clinical stage of disease<sup>57</sup>.

Microbleeds on the other hand have been found to predict mortality, due to their association with increased risk for cardiovascular events and cardiovascular mortality<sup>58</sup>. MR imaging with correlative histopathologic examination showed hemosiderin deposits. Therefore, the hypointense contrast on MRI is hypothesized to be attributed to ferromagnetic iron present after hemosiderin breakdown at the haemorrhagic site<sup>59</sup>. Additionally, there was a strong association between MRI-observed microbleeds and CMIs, indicative of a shared underlying pathophysiologic mechanism, suggested to be CAA<sup>60</sup>.

Finally, CMIs are considered to be the most widespread vascular component of SVD and occur in 43% of AD patients, and are associated with lower cognitive performance<sup>61</sup>. Due to their small size, CMIs typically go undetected on MRI. However, a study by van Veluw et al. confirmed that via ex vivo T2 7T MRI, CMIs can be detected as hyperintense focal lesions if CMI size is larger than 0.5mm. Upon histological analysis, the on MRI visible CMIs appeared as pallor focal lesions of cellular death, attributed to ischemia<sup>62</sup>. Consequently, the authors explored in vivo detection of CMIs using 7T MRI. Although CMIs could be detected, resolution was decreased and only CMIs larger than 1 mm could be identified on MRI<sup>62</sup>. These results were confirmed

in a study by Niwa et al, in which only 33% of the histologically visible CMIs were observed on 3T MRI, none of which were smaller than 1mm<sup>54</sup>. With the knowledge on how and where to look for CMIs, this research has subsequently been taken to the in-vivo setting. At 3T, some CMIs were visualized and associated with cognitive impairment and dementia<sup>63,64</sup>.

In summary, MRI-pathology studies in AD provide insights into the pathogenic components of AD and the role iron plays in the contrast seen on susceptibility weighted sequences at ultra-high field MRI. Additionally, a translation from the post-mortem setting to the in-vivo setting was made in the ability to detect CMIs that are related to the clinical phenotype of AD. An excellent example of the full circle as visualized in Fig. 1. However, clinical applicability beyond the research setting, is still to be evaluated.

## Post-mortem MRI and histology in Parkinson's disease

Parkinson's disease (PD) is a neurodegenerative disorder with neural aggregates containing alpha-synuclein ( $\alpha$ -syn), named Lewy bodies (LB) and Lewy neurites (LN), as its pathological hallmark<sup>65</sup>. The subthalamic nucleus (STN), substantia nigra (SN) and locus coeruleus (LC) are nuclei of interest for treatment (STN) and diagnosing PD and related disorders. Unfortunately, these structures and their subcomponents have been, due to their small size, difficult to visualize with conventional MRI sequences at standard field strength. However, with increasing field strength and advanced MRI sequences, an increased anatomical accuracy is possible<sup>66</sup>. As such, early detection of SN degeneration or differential diagnosis based on these anatomical locations may now be possible. We will discuss these advancements in the following paragraphs.

### *Anatomy of the subthalamic nucleus*

Combined post-mortem imaging and histology studies in PD are still scarce. Most studies have focussed on imaging the subthalamic nucleus (STN) with subsequent histology to evaluate its anatomy<sup>67-69</sup> and usability as target for deep brain stimulation (DBS) in PD<sup>68,70,71</sup>. Initial studies were set up to define MRI based criteria for DBS electrode placement, for instance correlating T2-w hyposignal in the subthalamic region to iron content in the STN<sup>67</sup>. Nevertheless, using conventional MRI sequences such as T2-w, the STN is not clearly defined, which was confirmed by pathological reports of inaccuracies in electrode placement<sup>72</sup>. However, at 9.4T MRI with subsequent histological validation, the anatomical borders of the STN are much more clearly defined and significant anatomical variability is apparent<sup>69</sup>.

In turn, Al-Helli and colleagues used post-mortem 9.4T MRI and histology to assess the anatomical accuracy of lead placement after MRI-guided, MRI-verified STN DBS<sup>70</sup>. DBS is used in selected patients with PD when a reduced quality of life is the result of insufficient improvement of (motor) symptoms after medical management

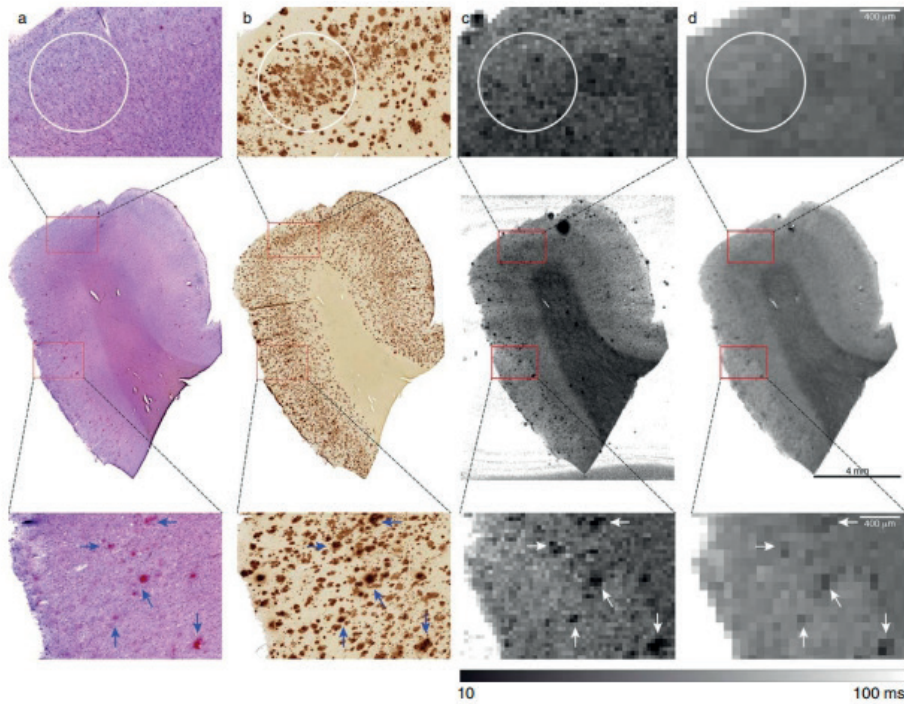


**Fig. 3 atching of 7T MRI and A $\beta$  histology.** Co-registration of (a) Congo Red and (b) A $\beta$  stains with corresponding quantitative (c) T2\* and (d) T2 maps. No signal decrease was observed corresponding to the outline of areas with A $\beta$  lacking CR positivity (white circle). In contrast, as an example several but not all amyloid plaques highlighted by the presence of both CR and A $\beta$  clearly resulted in hypo-intensities seen on the corresponding MR images (arrows). Reprint with permission from IOS Press<sup>45</sup>.

alone. The gold standard for verification of the anatomical location of electrodes is post-mortem<sup>73,74</sup>. Al-Helli and colleagues fixed brain tissue with the electrode still in situ, to keep the integrity of the tissue as intact as possible. They only removed the electrodes before MRI scanning, during which they were able to visualize the tract and lead placement, in different (MRI) planes. On T2-w 9.4T MRI, the electrode tracts were clearly visible as a hypointense rings, reaching the STN. Subsequently they used histology to visualize the electrode tracks which showed lymphocytes, gliosis, microglia, and macrophages in its surrounding tissue. They conclude a good correspondence between the two different modalities (MRI and histology) and that an MRI-guided, MRI-verified approach for DBS can accurately target the STN<sup>70</sup>.

### *Imaging the substantia nigra*

Other studies focussed more on assessing the ability to detect disease specific changes with MRI, such as visualization of the SN and associated dopaminergic cell loss in this region. A post-mortem MRI and pathology study with conventional T1-w imaging at 3T showed that hyperintense areas in the SN pars compacta (SNpc) of



a control donor were related to the presence of neuromelanin-containing neurons, while the iso-intense areas in the SNpc in PD and Dementia with Lewy Body (DLB) were related to a loss of neuromelanin-containing neurons.<sup>75</sup> Especially the nigrosomes, substructures of the SNpc, undergo extensive dopaminergic cell loss. Pathological studies show that cells of nigrosome 1 (N1) are affected in the early stages of PD, sequentially followed by cells in N2, N4, N3 and finally N5 in the later disease stages<sup>76</sup>.

Blazejewska and colleagues showed that visualization of nigrosome 1 within the SNpc is possible with 7T MRI. They scanned post-mortem midbrains from 2 non-neurological controls and 1 PD patient with T2\* and subsequently stained the brain sections with Perl, a staining for iron and neuromelanin. A hyperintense area within the dorsolateral border of the SNpc was observed in the non-neurological cases. Histopathological this was a calbindin-negative region with dopaminergic cells (TH positive) inside a larger calbindin-positive area; the location of nigrosome 1. Following this, they scanned 10 PD patients and 8 age-matched healthy controls (HC) in vivo and observed that this previously identified hyperintense region was bilaterally absent in PD cases, while present in 7 out of 8 HC. They conclude that these post-mortem and in vivo changes may provide a tool for studying the detection and progression of PD<sup>77</sup>.

A more recent study also included the other nigrosome subregions of the SN, and used an even higher field strength of 9.4T with histological validation. They included 10 controls, 5 PD cases and 8 cases with progressive supranuclear palsy (PSP)<sup>78</sup>. Massey and colleagues were able to identify high signal structures in controls as nigrosomes and were able to delineate all five substructures. Additionally they showed that these high signal structures were still present in PD, indicating that even in the presence of dopaminergic cell loss, the distinctive compartmental patterns of nigrosomes are still preserved<sup>78</sup>, which is in accordance to the literature on PD pathology<sup>76,79</sup>. Furthermore, Massey and colleagues found that these high signal structures were absent in PSP, indicating destruction of the nigrosome compartments<sup>78</sup> and a possible differential biomarker between PD and PSP.

Knowledge gained from the above mentioned PA-MRI studies on nigrosomes, was followed up in-vivo, in which researchers tried to visualize all five nigrosomes in 26 PD cases and 15 HC at 7T MRI. Although all nigrosomes (N1-N5) could be identified, N1 was identified with highest confidence in HC and signal intensity was abnormal (lower) in all PD cases and correlated with the Unified PD Rating Scale (UPDRS), making this the most promising SN biomarker in PD<sup>80</sup>.

### *Imaging the locus coeruleus*

The LC, through its noradrenergic connections, has been implicated in neurodegenerative disorders<sup>81,82</sup>. Keren and colleagues visualized the LC at 7T MRI and showed the steps for optimizing MRI sequences (see Fig. 4)<sup>83</sup>. Optimization from

a sequence used in vivo at 3T to ex-vivo 7T is necessary as increasing the field strength lengthens the T1 time and converges longitudinal relaxation, often limiting tissue contrast. Additionally, effects of fixation needs to be taken into account as well<sup>84,85</sup>. The Keren study furthermore showed that MRI contrast in the LC is primarily driven by neuromelanin<sup>83</sup>. Subsequently, Priovoulos and colleagues further improved 7T MRI sequences for LC visualization in the clinical (research) setting<sup>86</sup>.

In summary, post-mortem MRI and histology in PD has mainly focused on a few small regions; the STN, SN and LC. The first as an important endpoint for DBS and the other two as a regions associated with dopaminergic and noradrenergic cell loss, for which MRI visualization would be a possible non-invasive biomarker. For both regions anatomical accuracy is limited at lower field strengths with conventional sequences, therefore much effort has been made in optimizing the anatomical accuracy with advanced, iron-related sequences at ultra-high field strength, using histology as a gold standard. Some initial steps have already been made in translating these findings back to the clinical (research) setting<sup>80,86</sup>. Future studies will have to show the usability of these accurate anatomical maps and signal changes in defining and monitoring disease progression in PD.

### **Traumatic brain injury and stroke**

A limited number of post-mortem MRI studies have been performed on traumatic brain injury (TBI) and stroke. One of the main reasons is that in vivo MRI is rarely performed in the acute stages of TBI due to time constraints and difficulties in actively monitoring the patient within a magnetic field<sup>87</sup>. For this reason, computed tomography (CT) is more commonly used. Nevertheless, there is convincing evidence that MRI is more sensitive than CT for TBI<sup>88,89</sup>, including an initial study by Jones and colleagues who investigated MRI, CT and neuropathology in direct comparison. Six patients with severe TBI had ante-mortem CT and post-mortem 1.0T MRI with neuropathological assessment. Their results showed that MRI detected ~23% of pathological lesions, while CT only detected ~5%, a difference that was more prominent in smaller sized lesions. Additionally, CT underestimated lesion size with approximately 50%, while T2 images more closely approximated pathological size than T1 images<sup>87</sup>. In stroke, a systematic review and meta-analysis in animals (rats, mice and baboons) also found that T2 imaging was most effective for estimating infarct size, based on histological comparison<sup>90</sup>.

In the study by Jones et al, non-haemorrhagic lesion of diffuse axonal injury (DAI) were not detected by CT or by conventional low field-strength MRI sequences. More recent studies at higher field strength that also include haemorrhagic lesions, have looked at apparent diffusion coefficient (ADC) maps for depicting brain ischemia, and found a 73-92% sensitivity in the first three hours and 95-100% in the first six

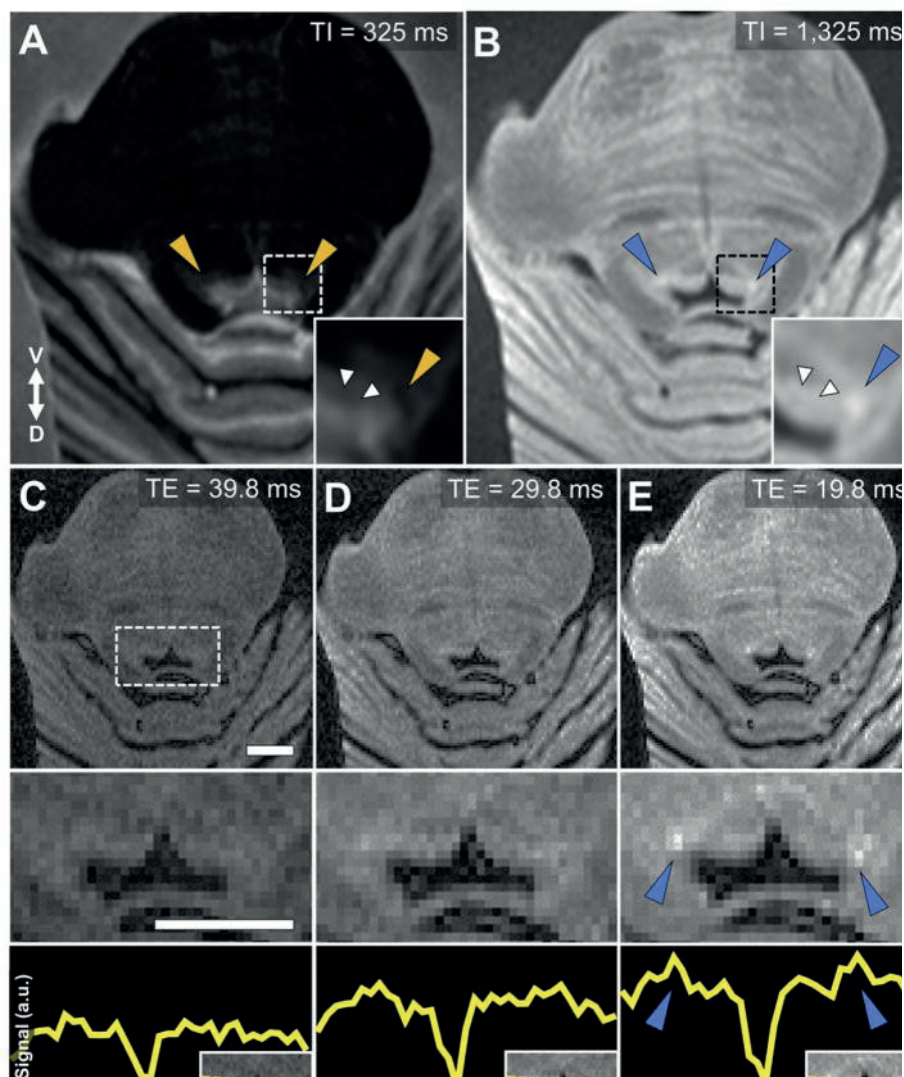


**Fig. 4 Optimal parameters for ex-vivo LC-MRI.** A rapid acquisition with refocused echoes (RARE) sequence was used to obtain axial sections from brainstem tissue embedded in agar. A) A short inversion recovery time (TI) produces distinct periaqueductal gray (PAG) contrast compared to surrounding tissue, but no elevated contrast in putative LC regions (orange triangles). B) Elevated contrast is still observed in the PAG with a long TI, as well as specific increased contrast in putative LC regions (blue triangles). C–E) A short echo time (TE) resulted in diminished PAG contrast relative to increased contrast in LC (blue triangles). Magnified 4th ventricular area (dashed box) is presented in the middle row. Bottom row demonstrates the relative increase in LC-MRI contrast with shorter TE using a linear ROI that was used to collect contrast values across the brainstem for each TE acquisition (y-axis: arbitrary units). An axial slice from the same tissue sample (HB 24) is presented in all images (ROI positioning shown in the inset at bottom right). Image parameters common across scans: number of slices = 8, slice thickness = 2 mm, slice spacing = 0.5 mm, repetition time = 3000 msec, inversion time = 825 ms, number of averages = 3, imaging resonance frequency = 300 MHz, echo train length = 2, flip angle = 180°, matrix size = 128 × 128, field of view = 4.00 × 4.00 cm, in-plane voxel size = 310 μm. Scale bars = 5 mm. Reprint with permission from Elsevier<sup>83</sup>.

hours<sup>89</sup>. In a rat model the spatiotemporal progression of ADC of water was further investigated, showing an early decrease in ADC (when CT and T2 are still normal), then 'pseudo-normalization' with an subsequent ADC increase due to cell lysis and necrosis<sup>89,91</sup>. Nevertheless, human post-mortem MRI validation studies are still lacking, but could be considered valuable to better understand the influence of stroke on surrounding tissue and how this may be reflected on MRI.

Repetitive TBI may lead to a progressive degenerative disorder named chronic traumatic encephalopathy (CTE). Pathological findings in CTE consist of the accumulation of hyperphosphorylated tau (p-tau), myelin loss, axonal injury and WM degeneration<sup>92</sup>. Holleran and colleagues tested the hypothesis that diffusion MRI might be useful for detecting WM microstructural changes in areas near tau pathology. They scanned formalin fixed tissue blocks of pathologically defined CTE patients with 11.4T MRI with subsequent histological assessment for (p-)tau and axonal disruption. Their results show that fractional anisotropy (FA) was associated with WM axonal damage, which was more pronounced in regions with adjacent GM (p-)tau pathology. They conclude that ex vivo diffusion MRI is sensitive for microstructural changes in CTE, but that application for the in vivo setting has yet to be determined<sup>92</sup>. Nevertheless, initial in vivo studies, show promising results<sup>93</sup>.

### **Summary, discussion and future prospects**

This review has given an overview of studies combining post-mortem MRI and histology in MS, AD and PD. Not only to better visualize anatomy and pathology, but also how this knowledge could be applied in the clinical setting.

In MS, the aim was mostly on being able to differentiate demyelinating lesions from areas of remyelination, and improving visualization of gray matter lesions. Pathological distinction of WM lesion types with quantitative MRI had many overlapping values, hence limiting clinical applicability<sup>18,19</sup>. Future studies at high or ultra-high field strength may bring better differentiation with more clinical usability to the table. Regarding visualization of gray matter lesion, retrospective inspection (with histopathological knowledge of lesion type and location), visualized up to ~80% of lesions, in contrast to the ~30% at prospective inspection<sup>32</sup>. Therefore, researchers suggest that training sessions with histological validation could possibly decrease this discrepancy for future studies and perhaps clinical practice<sup>32</sup>.

In AD, initial studies focussed on visualization of A $\beta$  pathology (through T2\* signal changes) with smaller tissue samples at increasing field strengths<sup>42,45</sup>. The possible clinical (research) applicability of these signal changes only became apparent in later years, when post-mortem differentiation between early and late onset AD could be made<sup>47</sup>. An excellent example of succesful translation from post-mortem MRI to the clinical research setting is the visualization of CMIs; detection of CMIs as hyperintense

focal lesions on ex vivo 7T MRI with histopathological validation<sup>62</sup>, then detection of CMLs on in vivo 7T MRI in the same study<sup>62</sup>, and subsequently on in vivo 3T MRI<sup>63,64</sup>, which could be related to clinical phenotype (cognitive impairment)<sup>63,64</sup>.

In PD, post-mortem imaging studies mainly involved obtaining a higher anatomical visualization of the STN, SN and LC. Clinical value is directly apparent for the STN, as better visualization of its borders is paramount for effective DBS<sup>69,70</sup>. For the SN and LC, post-mortem MRI and histology studies are making first strides towards the potential of using these locations as MRI biomarkers in differentiating diseases (PD or PSP)<sup>78</sup> or disease stages (sequential degeneration of nigrosomes)<sup>76,78</sup>. Nevertheless, replication in larger in vivo cohorts is required to better assess its clinical implementation value.

In TBI, studies combining post-mortem MRI and histology are still few, which may be due to the preference of CT above MRI in the clinical setting, as severely injured patients cannot be actively monitored in the proximity of a strong magnet. Nevertheless, the available post-mortem MRI and histology studies showed that MRI is more sensitive than CT for lesion (size)<sup>87</sup> and diffusion MRI is sensitive for detecting subtle microstructural changes, such as axonal disruption<sup>92</sup>. These are promising results which may have clinical value for patients not in the acute phase of TBI, e.g. monitoring of recovery.

The above paragraphs show that for both MS gray matter lesions, as well as AD related CMLs, not necessarily developing or optimizing MRI sequences, but training of MRI users, is more important for clinical implementation (Fig. 1). CMLs were very likely already visible on in vivo 3T MRI, but it's difficult to find them if you don't know where to look for. Knowing where to look, by looking at ultra-high field MRI with histological validation, is teaching researchers, and perhaps in future also radiologists, to better gauge where to look for at clinical resolution and field strength MRI. Perhaps PD research, which often focusses on small brainstem nuclei, could benefit from this knowledge in translating post-mortem MRI findings to clinical practice.

While MS and AD studies focused on visualizing pathology in specific cortical regions, PD studies were initially left behind due to difficulty in visualizing the small anatomical (sub)structures in the brainstem. By increasing the field strength and using more advanced MRI sequences, an increased anatomical accuracy became possible. The use of a reliable anatomical atlas is crucial for any subsequent clinical investigation. Therefore, the combination of post-mortem MRI and histology has played an important role in creating and validating several (cortical and subcortical) anatomical atlases<sup>71,94,95</sup>, or software packages<sup>96</sup>. Some based on a single brain<sup>94,95</sup>, and others on multiple brain specimens<sup>97</sup>. A recent development is not only including histology and multimodal MRI, but also structural connectivity to include tractography based parcellation<sup>71</sup>. This approach is especially interesting in defining DBS targets and assessing their projections.

The studies mentioned in this review show various MRI sensitivities for a variety of pathological hallmarks such as (cortical) demyelination, dopaminergic cell loss or deposits of fibrillary A $\beta$ . Nevertheless, while these images can visualize the presence or absence of pathology, they are not very pathologically specific; T2\* imaging appears to be the optimal sequence for all of the above mentioned pathological hallmarks. However, with considerable clinical heterogeneity in neurodegenerative disease and substantial discrepancies between clinical diagnosis relative to pathology,<sup>34,98,99</sup> it is not only imperative to be pathologically sensitive, but also pathologically specific.

Currently, conventional imaging techniques (e.g. T1-w or T2-w MRI) are too insensitive to pick up on disease specific subtleties; many cortical lesions are still missed in MS, and in AD and PD generally no cortical changes are observed with conventional MRI. Therefore, these studies may benefit from a more quantitative MRI approach, such as relaxometry, quantitative susceptibility mapping (QSM), diffusion tensor (DT) or magnetization transfer (MT) imaging combined with pathology, as these quantitative measures may be more pathologically specific. In regards to iron deposition quantification in vivo, QSM has become the preferred approach<sup>100</sup>, but has yet to be verified post-mortem. Additionally, these qMRI techniques could exploratively be used towards deep learning techniques to pick up subtleties even better than the human eye can do<sup>101,102</sup>.

Nevertheless, even post-mortem MRI and pathology studies have their limitations. Both post-mortem delay (PMD) and formalin fixation has an effect on MRI relaxometry<sup>84,85</sup>, therefore direct comparison between the post-mortem and in vivo setting is generally not possible. Nevertheless, when using quantitative MRI, relative comparison seems feasible; MT ratio of cortical MS lesions compared to surrounding normal appearing gray matter is lower both post-mortem and in vivo,<sup>103,104</sup> and dichotomous signal intensities (hyper- or hypointense) do not seem to change between the post-mortem and in vivo setting<sup>62,64,77</sup>. Additionally, although a comparison of ante-mortem and post-mortem MRI in humans is lacking, a study in rodents showed no significant changes in volumetric measurements of anatomical structures<sup>105</sup>.

A post-mortem study in forensic medicine furthermore shows that not only PMD, but also cause of death has a differential impact on diffusion measures; apparent diffusion coefficients (ADCs) were significantly lower in mechanical and hypoxic brain injury than in brains from subjects having died from heart failure<sup>106</sup>, something that researchers should take into account when studying donors with different causes of death. Although longitudinal MRI-pathology studies are not possible to following signal changes due to pathological changes over time, it may be feasible to obtain donors at different stages of disease<sup>107</sup>, or use an in-vivo derivative of pathology such as A $\beta$  Positron-emission tomography (PET) imaging, previously validated with post-mortem MRI and histology<sup>108</sup>. Furthermore, availability of

samples for post-mortem MRI and histology may be limited, sometimes due to the low prevalence of the disease. In those cases collaboration with multiple international brain banks may aid researchers, although uniformity in tissue collection is required.

This review has shown various ways in which post-mortem MRI and pathology has supported clinical research, not only by validating sequences, but also by coming up with suggestions for clinical implementation. Some have shown to be quite successful<sup>30,62</sup>, while others require further validation before implementation<sup>77</sup>. In conclusion, there is much to gain from post-mortem MRI and pathology studies, which should be further explored as new clinical questions emerge on the horizon.

## References

1. Josephs, K. A. et al. Rates of hippocampal atrophy and presence of post-mortem TDP-43 in patients with Alzheimer's disease: a longitudinal retrospective study. *Lancet Neurol.* 16, 917–924 (2017).
2. Kantarci, K. et al. White-matter integrity on DTI and the pathologic staging of Alzheimer's disease. *Neurobiol. Aging* (2017) doi:10.1016/j.neurobiolaging.2017.04.024.
3. Nedelska, Z. et al. Pattern of brain atrophy rates in autopsy-confirmed dementia with Lewy bodies. *Neurobiol. Aging* 36, 452–461 (2015).
4. Raman, M. R. et al. Antemortem MRI findings associated with microinfarcts at autopsy. *Neurology* 82, 1951–1958 (2014).
5. Petzold, A., Tozer, D. J. & Schmierer, K. Axonal damage in the making: neurofilament phosphorylation, proton mobility and magnetisation transfer in multiple sclerosis normal appearing white matter. *Exp. Neurol.* 232, 234–9 (2011).
6. Seehaus, A. K. et al. Histological Validation of DW-MRI Tractography in Human Postmortem Tissue. *Cereb. Cortex* 23, 442–450 (2013).
7. Hametner, S. et al. The influence of brain iron and myelin on magnetic susceptibility and effective transverse relaxation - A biochemical and histological validation study. *Neuroimage* 179, 117–133 (2018).
8. Meijer, F. J. A. & Goraj, B. Brain MRI in Parkinson's disease. *Front. Biosci. (Elite Ed)*. 6, 360–9 (2014).
9. Bell, J. E. et al. Management of a twenty-first century brain bank: experience in the BrainNet Europe consortium. *Acta Neuropathol.* 115, 497–507 (2008).
10. Samarasekera, N. et al. Brain banking for neurological disorders. *Lancet Neurol.* 12, 1096–1105 (2013).
11. Beach, T. G. et al. Arizona Study of Aging and Neurodegenerative Disorders and Brain and Body Donation Program. *Neuropathology* 35, 354–389 (2015).
12. Jonkman, L. E. & Geurts, J. J. G. Postmortem magnetic resonance imaging in Handbook of clinical neurology vol. 150 335–354 (2018).
13. Seewann, A. et al. Translating pathology in multiple sclerosis: the combination of postmortem imaging, histopathology and clinical findings. *Acta Neurol. Scand.* 119, 349–55 (2009).
14. Lassmann, H. Recent neuropathological findings in MS—implications for diagnosis and therapy. *J. Neurol.* 251 Suppl, IV2-5 (2004).
15. Lucchinetti, C., Brück, W. & Noseworthy, J. Multiple sclerosis: recent developments in neuropathology, pathogenesis, magnetic resonance imaging studies and treatment. *Curr. Opin. Neurol.* 14, 259–69 (2001).
16. Matthews, P. M. & Arnold, D. L. Magnetic resonance imaging of multiple sclerosis: new insights linking pathology to clinical evolution. *Curr. Opin. Neurol.* 14, 279–87 (2001).
17. Miller, D. H., Grossman, R. I., Reingold, S. C. & McFarland, H. F. The role of magnetic resonance techniques in understanding and managing multiple sclerosis. *Brain* 121 ( Pt 1, 3–24 (1998).
18. Barkhof, F. et al. Remyelinated lesions in multiple sclerosis: magnetic resonance image appearance. *Arch. Neurol.* 60, 1073–81 (2003).
19. Zhang, Y. et al. Multi-scale MRI spectrum detects differences in myelin integrity between MS lesion types. *Mult. Scler.* (2016) doi:10.1177/1352458515624771.
20. Yao, B. et al. Chronic Multiple Sclerosis Lesions: Characterization with High-Field-Strength MR Imaging. (2012).
21. Wegner, C., Esiri, M. M., Chance, S. A., Palace, J. & Matthews, P. M. Neocortical neuronal, synaptic, and glial loss in multiple sclerosis. *Neurology* 67, 960–7 (2006).
22. Peterson, J. W., Bö, L., Mörk, S., Chang, A. & Trapp, B. D. Transected neurites, apoptotic neurons, and reduced inflammation in cortical multiple sclerosis lesions. *Ann. Neurol.* 50, 389–400 (2001).
23. Calabrese, M. et al. Cortical diffusion-tensor imaging abnormalities in multiple



- sclerosis: a 3-year longitudinal study. *Radiology* 261, 891–8 (2011).
24. Roosendaal, S. D. et al. In vivo MR imaging of hippocampal lesions in multiple sclerosis. *J. Magn. Reson. Imaging* 27, 726–31 (2008).
  25. Roosendaal, S. D. et al. Accumulation of cortical lesions in MS: relation with cognitive impairment. *Mult. Scler.* 15, 708–14 (2009).
  26. Kidd, D. et al. Cortical lesions in multiple sclerosis. *Brain* 122 ( Pt 1, 17–26 (1999).
  27. Geurts, J. J. G. et al. Cortical lesions in multiple sclerosis: combined postmortem MR imaging and histopathology. *AJNR. Am. J. Neuroradiol.* 26, 572–7 (2005).
  28. Seewann, A. et al. Postmortem verification of MS cortical lesion detection with 3D DIR. *Neurology* 78, 302–8 (2012).
  29. Simon, B. et al. Improved in vivo detection of cortical lesions in multiple sclerosis using double inversion recovery MR imaging at 3 Tesla. *Eur. Radiol.* 20, 1675–83 (2010).
  30. Geurts, J. J. G. et al. Consensus recommendations for MS cortical lesion scoring using double inversion recovery MRI. *Neurology* 76, 418–24 (2011).
  31. Kilsdonk, I. D. et al. Increased cortical grey matter lesion detection in multiple sclerosis with 7 T MRI: a post-mortem verification study. *Brain* (2016) doi:10.1093/brain/aww037.
  32. Jonkman, L. E., Klaver, R., Fleysler, L., Inglesse, M. & Geurts, J. J. G. Ultra-High-Field MRI Visualization of Cortical Multiple Sclerosis Lesions with T2 and T2\*: A Postmortem MRI and Histopathology Study. *AJNR. Am. J. Neuroradiol.* (2015) doi:10.3174/ajnr.A4418.
  33. Pitt, D. et al. Imaging cortical lesions in multiple sclerosis with ultra-high-field magnetic resonance imaging. *Arch. Neurol.* 67, 812–8 (2010).
  34. Beach, T. G., Monsell, S. E., Phillips, L. E. & Kukull, W. Accuracy of the clinical diagnosis of Alzheimer disease at National Institute on Aging Alzheimer Disease Centers, 2005-2010. *J. Neuropathol. Exp. Neurol.* 71, 266–73 (2012).
  35. Apostolova, L. G. et al. Relationship between hippocampal atrophy and neuropathology markers: A 7T MRI validation study of the EADC-ADNI Harmonized Hippocampal Segmentation Protocol. *Alzheimer's Dement.* 11, 139–150 (2015).
  36. Apostolova, L. G. et al. Subregional hippocampal atrophy predicts Alzheimer's dementia in the cognitively normal. *Neurobiol. Aging* 31, 1077–1088 (2010).
  37. De Leon, M. J. et al. Frequency of hippocampal formation atrophy in normal aging and Alzheimer's disease. *Neurobiol. Aging* 18, 1–11 (1997).
  38. Apostolova, L. G. et al. 3D comparison of hippocampal atrophy in amnesic mild cognitive impairment and Alzheimer's disease. *Brain* 129, 2867–2873 (2006).
  39. Apostolova, L. G. et al. Conversion of Mild Cognitive Impairment to Alzheimer Disease Predicted by Hippocampal Atrophy Maps. *Arch. Neurol.* 63, 693 (2006).
  40. Jack, C. R. et al. Antemortem MRI findings correlate with hippocampal neuropathology in typical aging and dementia. *Neurology* 58, 750–7 (2002).
  41. Giuliano, A. et al. Hippocampal subfields at ultra high field MRI: An overview of segmentation and measurement methods. *Hippocampus* 27, 481–494 (2017).
  42. Benveniste, H., Einstein, G., Kim, K. R., Hulette, C. & Johnson, G. A. Detection of neuritic plaques in Alzheimer's disease by magnetic resonance microscopy. *Proc. Natl. Acad. Sci. U. S. A.* 96, 14079–84 (1999).
  43. Meadowcroft, M. D., Connor, J. R., Smith, M. B. & Yang, Q. X. MRI and Histological Analysis of Beta-Amyloid Plaques in Both Human Alzheimer's Disease and APP/PS1 Transgenic Mice. *J. Magn. Reson. Imaging* (2009) doi:10.1002/jmri.21731.
  44. Nabuurs, R. J. A. et al. High-field MRI of single histological slices using an inductively coupled, self-resonant microcoil: Application to ex vivo samples of patients with Alzheimer's disease. *NMR Biomed.* (2011) doi:10.1002/nbm.1598.

45. Nabuurs, R. J. A. et al. MR microscopy of human amyloid- $\beta$  deposits: Characterization of parenchymal amyloid, diffuse plaques, and vascular amyloid. *J. Alzheimer's Dis.* 34, 1037–1049 (2013).
46. Zeineh, M. M. et al. Activated iron-containing microglia in the human hippocampus identified by magnetic resonance imaging in Alzheimer disease. *Neurobiol. Aging* 36, 2483–2500 (2015).
47. Bulk, M. et al. Postmortem MRI and histology demonstrate differential iron accumulation and cortical myelin organization in early- and late-onset Alzheimer's disease. *Neurobiol. Aging* 62, 231–242 (2018).
48. Kenkhuis, B. et al. 7T MRI allows detection of disturbed cortical lamination in medial temporal lobe in patients with Alzheimer's disease. Submitted (2018).
49. Attems, J. & Jellinger, K. A. The overlap between vascular disease and Alzheimer's disease—lessons from pathology. *BMC Med.* 12, 206 (2014).
50. Pantoni, L. Cerebral small vessel disease: from pathogenesis and clinical characteristics to therapeutic challenges. *Lancet. Neurol.* 9, 689–701 (2010).
51. Attems, J. & Jellinger, K. A. The overlap between vascular disease and Alzheimer's disease - lessons from pathology. *BMC Med.* 12, 206 (2014).
52. Kövari, E., Herrmann, F. R., Hof, P. R. & Bouras, C. The relationship between cerebral amyloid angiopathy and cortical microinfarcts in brain ageing and Alzheimer's disease. *Neuropathol. Appl. Neurobiol.* 39, 498–509 (2013).
53. Soontornniyomkij, V. et al. Cerebral Microinfarcts Associated with Severe Cerebral  $\beta$ -Amyloid Angiopathy. *Brain Pathol.* 20, 459–467 (2010).
54. Niwa, A. et al. Comparative Analysis of Cortical Microinfarcts and Microbleeds using 3.0-Tesla Postmortem Magnetic Resonance Images and Histopathology. *J. Alzheimer's Dis.* 59, 951–959 (2017).
55. De Reuck, J. L. et al. The Significance of Cortical Cerebellar Microbleeds and Microinfarcts in Neurodegenerative and Cerebrovascular Diseases. *Cerebrovasc. Dis.* 39, 138–143 (2015).
56. Fazekas, F. et al. Pathologic correlates of incidental MRI white matter signal hyperintensities. *Neurology* 43, 1683–9 (1993).
57. Mortamais, M., Artero, S. & Ritchie, K. White matter hyperintensities as early and independent predictors of Alzheimer's disease risk. *J. Alzheimers. Dis.* 42 Suppl 4, S393-400 (2014).
58. Benedictus, M. R. et al. Microbleeds, Mortality, and Stroke in Alzheimer Disease. *JAMA Neurol.* 72, 539 (2015).
59. Fazekas, F. et al. Histopathologic analysis of foci of signal loss on gradient-echo T2\*-weighted MR images in patients with spontaneous intracerebral hemorrhage: evidence of microangiopathy-related microbleeds. *AJNR. Am. J. Neuroradiol.* 20, 637–42 (1999).
60. Lauer, A. et al. Microbleeds on MRI are associated with microinfarcts on autopsy in cerebral amyloid angiopathy. *Neurology* 87, 1488–1492 (2016).
61. Brundel, M., de Bresser, J., van Dillen, J. J., Kappelle, L. J. & Biessels, G. J. Cerebral Microinfarcts: A Systematic Review of Neuropathological Studies. *J. Cereb. Blood Flow Metab.* 32, 425–436 (2012).
62. van Veluw, S. J. et al. In Vivo Detection of Cerebral Cortical Microinfarcts with High-Resolution 7T MRI. *J. Cereb. Blood Flow Metab.* 33, 322–329 (2013).
63. Hilal, S. et al. Cortical cerebral microinfarcts on 3T MRI. *Neurology* 87, 1583–1590 (2016).
64. Ferro, D. A. et al. Cortical Cerebral Microinfarcts on 3 Tesla MRI in Patients with Vascular Cognitive Impairment. *J. Alzheimer's Dis.* 60, 1443–1450 (2017).
65. Braak, H. et al. Staging of brain pathology related to sporadic Parkinson's disease. *Neurobiol. Aging* 24, 197–211.
66. Massey, L. A. & Yousry, T. A. Anatomy of the Substantia Nigra and Subthalamic Nucleus on MR Imaging. *Neuroimaging Clin. N. Am.* 20, 7–27 (2010).
67. Dormont, D. et al. Is the subthalamic nucleus hypointense on T2-weighted images? A correlation study using MR

- imaging and stereotactic atlas data. *AJNR. Am. J. Neuroradiol.* 25, 1516–23 (2004).
68. Rijkers, K. et al. The microanatomical environment of the subthalamic nucleus. *J. Neurosurg.* 107, 198–201 (2007).
69. Massey, L. A. et al. High resolution MR anatomy of the subthalamic nucleus: Imaging at 9.4T with histological validation. *Neuroimage* 59, 2035–2044 (2012).
70. Al-Helli, O. et al. Deep brain stimulation of the subthalamic nucleus: histological verification and 9.4-T MRI correlation. *Acta Neurochir. (Wien).* 157, 2143–2147 (2015).
71. Ewert, S. et al. Toward defining deep brain stimulation targets in MNI space: A subcortical atlas based on multimodal MRI, histology and structural connectivity. *Neuroimage* 170, 271–282 (2018).
72. McClelland, S. et al. Relationship of clinical efficacy to postmortem-determined anatomic subthalamic stimulation in Parkinson syndrome. *Clin. Neuropathol.* 26, 267–75.
73. Vedam-Mai, V., Yachnis, A., Ullman, M., Javedan, S. P. & Okun, M. S. Postmortem observation of collagenous lead tip region fibrosis as a rare complication of DBS. *Mov. Disord.* 27, 565–569 (2012).
74. Sun, D. A. et al. Postmortem analysis following 71 months of deep brain stimulation of the subthalamic nucleus for Parkinson disease. *J. Neurosurg.* 109, 325–329 (2008).
75. Kitao, S. et al. Correlation between pathology and neuromelanin MR imaging in Parkinson's disease and dementia with Lewy bodies. *Neuroradiology* 55, 947–953 (2013).
76. Damier, P., Hirsch, E. C., Agid, Y. & Graybiel, A. M. The substantia nigra of the human brain. II. Patterns of loss of dopamine-containing neurons in Parkinson's disease. *Brain* 122 ( Pt 8), 1437–48 (1999).
77. Blazejewska, A. I. et al. Visualization of nigrosome 1 and its loss in PD: Pathoanatomical correlation and in vivo 7 T MRI. *Neurology* 81, 534–540 (2013).
78. Massey, L. A. et al. 9.4 T MR microscopy of the substantia nigra with pathological validation in controls and disease. *NeuroImage. Clin.* 13, 154–163 (2017).
79. Damier, P., Hirsch, E. C., Agid, Y. & Graybiel, A. M. The substantia nigra of the human brain. *Brain* 122, 1437–1448 (1999).
80. Schwarz, S. T. et al. Parkinson's disease related signal change in the nigrosomes 1–5 and the substantia nigra using T2\* weighted 7T MRI. *NeuroImage Clin.* 19, 683–689 (2018).
81. Zarow, C., Lyness, S. A., Mortimer, J. A. & Chui, H. C. Neuronal loss is greater in the locus coeruleus than nucleus basalis and substantia nigra in Alzheimer and Parkinson diseases. *Arch. Neurol.* 60, 337–41 (2003).
82. Vazey, E. M. & Aston-Jones, G. The emerging role of norepinephrine in cognitive dysfunctions of Parkinson's disease. *Front. Behav. Neurosci.* 6, 48 (2012).
83. Keren, N. I. et al. Histologic validation of locus coeruleus MRI contrast in post-mortem tissue. *Neuroimage* 113, 235–45 (2015).
84. Birkl, C. et al. Effects of formalin fixation and temperature on MR relaxation times in the human brain. *NMR Biomed.* 29, 458–465 (2016).
85. Shatil, A. S., Uddin, M. N., Matsuda, K. M. & Figley, C. R. Quantitative Ex Vivo MRI Changes due to Progressive Formalin Fixation in Whole Human Brain Specimens: Longitudinal Characterization of Diffusion, Relaxometry, and Myelin Water Fraction Measurements at 3T. *Front. Med.* 5, 31 (2018).
86. Priovoulos, N. et al. High-resolution in vivo imaging of human locus coeruleus by magnetization transfer MRI at 3T and 7T. *Neuroimage* 168, 427–436 (2018).
87. Jones, N. R. et al. Correlation of postmortem MRI and CT appearances with neuropathology in brain trauma: a comparison of two methods. *J. Clin. Neurosci.* 5, 73–9 (1998).
88. Hesselink, J. R. et al. MR imaging of brain contusions: a comparative study with CT. *AJR. Am. J. Roentgenol.* 150, 1133–42

- (1988).
89. Vilela, P. & Rowley, H. A. Brain ischemia: CT and MRI techniques in acute ischemic stroke. *Eur. J. Radiol.* 96, 162–172 (2017).
90. Milidonis, X., Marshall, I., Macleod, M. R. & Sena, E. S. Magnetic Resonance Imaging in Experimental Stroke and Comparison With Histology. *Stroke* 46, 843–851 (2015).
91. Knight, M. J. et al. A spatiotemporal theory for MRI  $T_2$  relaxation time and apparent diffusion coefficient in the brain during acute ischaemia: Application and validation in a rat acute stroke model. *J. Cereb. Blood Flow Metab.* 36, 1232–1243 (2016).
92. Holleran, L. et al. Axonal disruption in white matter underlying cortical sulcus tau pathology in chronic traumatic encephalopathy. *Acta Neuropathol.* 133, 367–380 (2017).
93. Ruprecht, R., Scheurer, E. & Lenz, C. Systematic review on the characterization of chronic traumatic encephalopathy by MRI and MRS. *J. Magn. Reson. Imaging* (2018) doi:10.1002/jmri.26162.
94. Yelnik, J. et al. A three-dimensional, histological and deformable atlas of the human basal ganglia. I. Atlas construction based on immunohistochemical and MRI data. *Neuroimage* 34, 618–638 (2007).
95. Chakravarty, M. M., Bertrand, G., Hodge, C. P., Sadikot, A. F. & Collins, D. L. The creation of a brain atlas for image guided neurosurgery using serial histological data. *Neuroimage* 30, 359–376 (2006).
96. Cardinale, F. et al. Validation of FreeSurfer-Estimated Brain Cortical Thickness: Comparison with Histologic Measurements. *Neuroinformatics* 12, 535–542 (2014).
97. Morel, A., Magnin, M. & Jeanmonod, D. Multiarchitectonic and stereotactic atlas of the human thalamus. *J. Comp. Neurol.* 387, 588–630 (1997).
98. Gaugler, J. E. et al. Characteristics of patients misdiagnosed with Alzheimer's disease and their medication use: an analysis of the NACC-UDS database. *BMC Geriatr.* 13, 137 (2013).
99. Rizzo, G. et al. Accuracy of clinical diagnosis of Parkinson disease. *Neurology* 86, 566–576 (2016).
100. Yan, F., He, N., Lin, H. & Li, R. Iron deposition quantification: Applications in the brain and liver. *J. Magn. Reson. Imaging* 48, 301–317 (2018).
101. Yoo, Y. et al. Deep learning of joint myelin and T1w MRI features in normal-appearing brain tissue to distinguish between multiple sclerosis patients and healthy controls. *NeuroImage Clin.* 17, 169–178 (2018).
102. Ambastha, A. K., Leong, T.-Y. & Alzheimer's Disease Neuroimaging Initiative. A Deep Learning Approach to Neuroanatomical Characterisation of Alzheimer's Disease. *Stud. Health Technol. Inform.* 245, 1249 (2017).
103. Jonkman, L. E. et al. Ultra-high field MTR and qR2\* differentiates subpial cortical lesions from normal-appearing gray matter in multiple sclerosis. *Mult. Scler.* (2015) doi:10.1177/1352458515620499.
104. Derakhshan, M., Caramanos, Z., Narayanan, S., Arnold, D. L. & Louis Collins, D. Surface-based analysis reveals regions of reduced cortical magnetization transfer ratio in patients with multiple sclerosis: a proposed method for imaging subpial demyelination. *Hum. Brain Mapp.* 35, 3402–13 (2014).
105. Oguz, I. et al. Comparison of Magnetic Resonance Imaging in Live vs. Post Mortem Rat Brains. *PLoS One* 8, e71027 (2013).
106. Scheurer, E. et al. Forensic Application of Postmortem Diffusion-Weighted and Diffusion Tensor MR Imaging of the Human Brain in Situ. *Am. J. Neuroradiol.* 32, 1518–1524 (2011).
107. Braak, H. & Braak, E. Neuropathological staging of Alzheimer-related changes. *Acta Neuropathol.* 82, 239–259 (1991).
108. Ikonomic, M. D. et al. Post-mortem correlates of in vivo PiB-PET amyloid imaging in a typical case of Alzheimer's disease. *Brain* 131, 1630–45 (2008).

